A Novel Method for Manipulating Flexible Cylinder Vortex-Induced Vibrations

Ersegun Deniz Gedikli*, David Chelidze, Jason Dahl*****
***Sustainable Arctic Marine and Coastal Technology (SAMCoT), Centre for Research-based Innovation (CRI), Norwegian University of Science and Technology (NTNU), Trondheim, Norway**, deniz.gedikli@ntnu.no
****Department of Mechanical, Industrial and Systems Engineering, University of Rhode Island, Kingston, RI, USA,** chelidze@uri.edu
*****Department of Ocean Engineering, University of Rhode Island, Narragansett, RI, USA**, jmdahl@uri.edu

Abstract

In this work, we developed a novel experimental method to suppress the motion of a flexible cylinder undergoing vortex-induced vibrations using piezoelectric stripe actuators. The test cylinder was made of urethane rubber and specific stiffness characteristics was provided by molding a beam through the center of the test cylinder. Experiments were conducted in the Experimental Fluid Mechanics Laboratory (EFML) located at the University of Rhode Island's Narragansett Bay campus. In the tests, small piezo electric patches were bonded at the second mode anti-node of the cylinder in the in-line (in-flow) direction. Results showed that if motion characteristics of the cylinder are identified carefully, one could significantly suppress the large cylinder motions by disrupting the frequency of the cylinder. In other words, small energy input in the in-line could potentially result a significant amplitude drop in combined in-line and cross-flow directions. In-line direction was chosen on purpose since in-line amplitudes are inherently lower than cross-flow amplitudes in vortex-induced vibrations therefore requires less energy to control.

Keywords: VIV, Flexible Cylinder, Control, Piezoelectric

1. Introduction

Vortex-induced vibration (VIV) can be described as an amplitude limited motion of structures that are subject to fluid flow. VIV is a serious problem in offshore structures and can cause serious problems. Such motions increase the fatigue characteristics of the structures, may decrease the operational time and may even result a catastrophic failure. Therefore, it is important to understand, and develop methods to control and predict these motions.

In the early studies, VIV was treated as a single degree of freedom spring mass dashpot problem where cylinder oscillated only in the cross-flow direction (Bearman, 1984; Sarpkaya, 2004; Williamson and Govardhan, 2004). However, studies such as Jauvtis and Williamson (2004), Dahl et al. (2006), Dahl et al. (2007) and many more showed that in-line motion may have a significant effect in the vibration and can increase the fatigue characteristics of the structures by orders of magnitude (Modarres-Sadeghi et al., 2010). Although, these studies provide insights into complex fluid-structure interactions, it is still unclear how much of these motions successfully represent the behaviour of long flexible cylinders. Because it is known that, the applications in offshore engineering are mostly related to the use of flexible cylinders (Huera-Huarte et al., 2014).

Previous studies on flexible cylinders involved both numerical (Bourguet et al., 2011a) and experimental (Vandiver, 1993; Chaplin et al., 2005; Vandiver et al. 2006; Huera.Huarte and Bearman, 2009; Gedikli and Dahl, 2014; Gedikli et al., 2017) studies. These studies illustrated the complex nature of fluid-structure interactions showing multi-modal type of behaviours in both in-line and cross-flow directions. In addition, Gedikli et al. (2017) and Gedikli and Dahl (2017) showed that specific mode combinations on a flexible cylinder are more or less likely to produce figure-eight type of motions. This is significant, because Dahl et al., 2007 had showed that high-harmonic forcing was associated with large figure eight type of responses, which possess significant danger to offshore structures due to the aforementioned reasons. Therefore, suppressing these undesirable motions of such systems is of utmost importance to the offshore industry for many years.

There have been a great effort developing control techniques to suppress VIV in the recent years. These methods can mainly divided into two categories as active and passive control methods. In passive control, no energy is required by the system to control the motion of the body. For example, changing the geometry of the structure may disturb the wake characteristics behind the cylinder and may reduce the vibration significantly. In fact, this method was very much liked by the offshore industry due to its easy implementation. Readers are encouraged to read Blevins (1990), for an extensive list of such popular systems (i.e. strouts, helical strakes, fairings and many more). Second method is active control methods where an energy input is required for vibration suppression. This method can be divided into two sub-categories as open-loop and closed-loop active control methods. In open-loop method, an external energy is provided by a source from outside to disturb the motion characteristics as in Cheng et al. (2003). In closed-loop method, a feedback mechanism can be developed as in Baz and Kim (1993), and Williams and Zhao (1989) for vibration suppression.

In this study, we develop a novel open-loop active control method to suppress flexible cylinder motions. The scientific question we are trying to answer is “If one identifies the structural characteristics carefully for a specific Reynolds number range, is it possible to disturb the frequency of the structure so that cylinder's amplitude could be reduced from a large amplitude state to a lower amplitude state?" To answer this question, we use a beam with specific structural characteristics and bond two piezo-electric patches at the second mode (full-sinusoid) anti-nodes of the test beam. Then, we mold a flexible cylinder with beam in the center using urethane rubber molding material to give it a circular shape. Later, we conduct two set of experiments in air and in water. By conducting the experiments in air, we characterize the cylinder motion in air, and test the hypothesis. Then, in the second phase, we conduct the experiments in the recirculating flow channel and test the hypothesis in water.

2. Description of the experimental method

Experiments were carried out at the EFM Laboratory located at the University of Rhode Island's Narragansett Bay campus. In the experiments, a bending dominated flexible cylinder was tested first in air, then in water.

2.1. Cylinder and piezo characteristics

Specific frequency and mode shape characteristics were ensured by molding a plastic beam through the centre of the test cylinder. To find the correct size of beam, the natural frequency equation for a fixed-fixed beam was used:

$$f_n = \frac{\lambda_n^2}{2\pi}\sqrt{\frac{EI}{ML^4}} \tag{1}$$

where $\lambda_n = (2n+1)\frac{\pi}{2}$, E is the elasticity of modulus, M is the mass per unity length, L is the cylinder length, and I is the area moment of inertia, n is the specific mode number (see Gedikli and Dahl, 2014). Since we are interested in large vibrations (i.e., vibrations around resonance), the natural frequency of the plastic beam was equated to the shedding frequency and specific beam characteristics were chosen based on the area moment of inertia of each test cylinder such that they all satisfy the in-line: cross-flow frequency ratio of 2. This is important because, large figure-eight motions are found to be associated with frequency ratio of 2 as shown in Dahl et al. (2006).

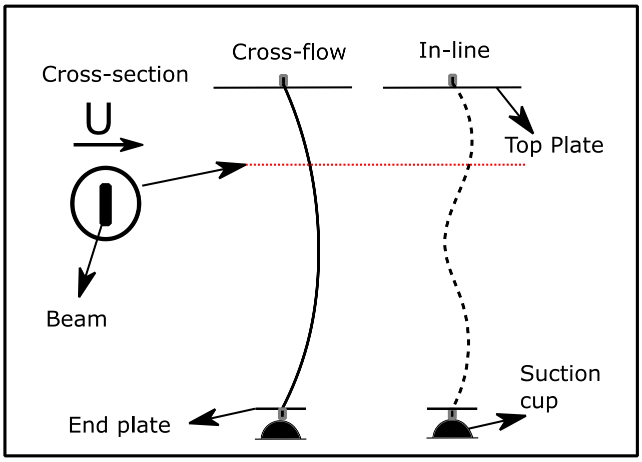

Fig. 1. Sketch of the cross-section of the test cylinder with the designed mode shapes in cross-flow and in-line directions.

The piezo patches used in the experiments were from Piezo Systems which had a length of 4.9 mm, width of a 2 mm and depth of 0.8 mm.

2.2. In-air experiments

In-air experiments were carried out using a shaker-rail apparatus developed in EFML as seen in the left image in Fig.1 where a shaker was connected to the rail system and the cylinder was attached to it vertically. Right image in Fig.1 illustrates the front view of the beam with piezoelectric patches bonded at the second mode anti-nodes of the cylinder.

Three set of experiments were carried out to characterize the response of the test cylinder and to control the specific motions. In the first experiments, the shaker was excited with a varying sinusoidal base excitations for increasing and decreasing shaker frequencies. Resulting motion characteristics were recorded at two locations using two laser displacement sensors (LDS) as shown in the left image in Fig.1. In the second set of experiments, the shaker was turned-off and only piezo responses were recorded for increased and decreased piezo frequencies.

Once the cylinder's natural response to varying base excitations and piezo-excited response at zero-base excitation were known, it was attempted to change the motion amplitude by using the shaker and piezo excitation simultaneously in the third set of experiments.

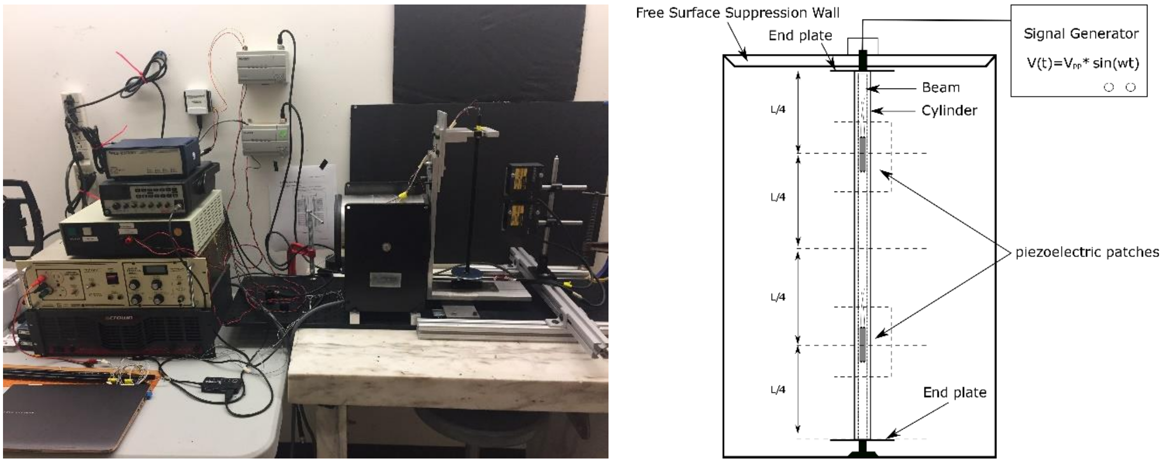

Fig. 2. Left image: Shaker-rail apparatus designed at the University of Rhode Island. Right image: Front view of the beam with piezoelectric patches in the recirculating flow channel.

2.3. In-water experiments

In-water experiments were carried out in a recirculating flow channel in the EFML located at the Narragansett Bay Campus of the University of Rhode Island. Fig.3 illustrates the in-line and cross-flow camera views along with a picture of the experimental set-up. The recirculating flow channel used in the experiments has three viewing windows at sides and one in the front for flow visualization. In the experiments, two high speed cameras were used (Phantom V10 series) where one of them was located in front of the flow channel to capture the motion in the cross-flow direction, the other one was located at the side of the tank to capture the motion in the in-line (in-flow) direction. In order to ensure the orthogonality between the cameras, a point laser was used for calibration. These cameras were capable of capturing images with 2400×1800 pixels of resolution, but maximum resolution was not used in the current experiments. Instead, cameras were re-adjusted to 800×1800 pixels of resolution, which helped to increase the time histories and decreased the saving time. Test cylinder was placed vertical to the incoming fluid flow. It was attached to the bottom viewing-window using a strong suction cup, and attached to the aluminium mechanism at the top. The aluminium mechanism consists of an upper aluminium body and a rectangle hard plastic plate covering the top of the tank under the free surface (with a small circular opening). The plate is adjustable and can move up and down so that one can adjust the height. At this point, the use of the plate is significant; because, first, it eliminates the free surface flow variations; secondly, it allows us to attach the cylinder at the top and last, it provides a symmetric flow pattern for the flow speed range tested.

Cylinder was marked with 22 equally spaced white dots in both in-line and cross-flow directions that are 1.6 cm apart from each other (see left and right images in Fig.2). Cameras recorded the cylinder motion with a frame rate of $150Hz$. A motion tracking software was used to analyze the motion of each marker on the cylinder. The software works based on subpixel accuracy and is capable of capturing the motion in two dimensions.

Fig. 3. Experimental set-up in flow channel. Left image: In-line camera view. Center image: Flow channel set-up. Right image: Cross-flow camera view.

Tests were carried out for increased and decreased Reynolds number values between 900-5200. Similar to in-air experiments first, amplitude characteristics of the test cylinder was analyzed. Then, maximum piezo frequency (found in in-air experiments) was activated at selected Reynold numbers to force the cylinder to change its modal response for vibration suppression.

It should also be remembered that, in the current experiments piezo patches were bonded in the in-line direction. The reason of this is that in-line amplitudes are inherently lower than cross-flow amplitudes; therefore, in-line modal change requires lower energy than cross-flow. However, since vortex-induced vibration is a complex coupled fluid-structure interaction, any change in in-line also affects the cross-flow response.

3. Results & Discussion

3.1. Piezo characteristics

Fig. 4 illustrates the normalized amplitude response for increased and decreased shaker frequencies. In this case, shaker frequency was varied providing a base excitation and corresponding response at the centre was analyzed. As one can see, cylinder reached the maximum amplitude of 4.2 at $6Hz$ for increased frequencies and reached close to 3 at $5Hz$ for decreased frequencies. A hysteretic type of response was observed between these two cases leading two different amplitude responses. Experiments were repeated for four times to ensure that the resulting amplitude response is stable over different experiments. A pluck test was also carried out to test the natural frequency of the cylinder, and the natural frequency was found to be close to $6Hz$ in air.

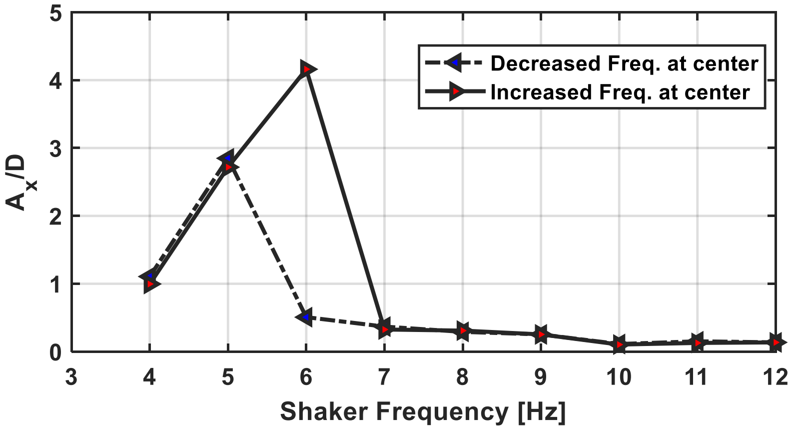

Fig. 4. Cylinder's center point amplitude response at center for increased and decreased shaker frequencies.

Then, piezo only response was analyzed for increased and decreased piezo frequencies. Fig. 5 shows the normalized amplitude response at center location of the cylinder. As one see, the test cylinder reached the maximum amplitude at $40Hz$ for increased and decreased frequencies. Although, a small hysteretic type of response was observed in the amplitudes, it did not change the fact that cylinder reached the maximum amplitude at the piezo frequency of $40Hz$, which was the sole purpose of this exercise (to see at what frequency cylinder reached the maximum amplitude).

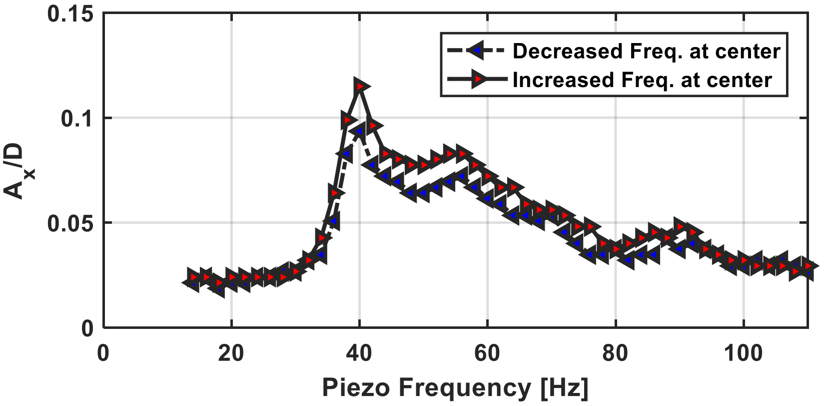

Fig. 5. Cylinder's center point amplitude response at center for increased and decreased piezo frequencies.

Since it is now known that piezo reaches the maximum amplitude at $40Hz$, and cylinder reaches the maximum amplitude at $6Hz$ (for increased case); one can activate the piezo frequency whilst the test cylinder is oscillating at its maximum amplitude. Fig. 6 illustrates such attempt where piezo was activated around 18 seconds to disrupt the oscillation frequency, which resulted a significant amplitude drop. This illustration showed that, the proposed hypothesis is working in air.

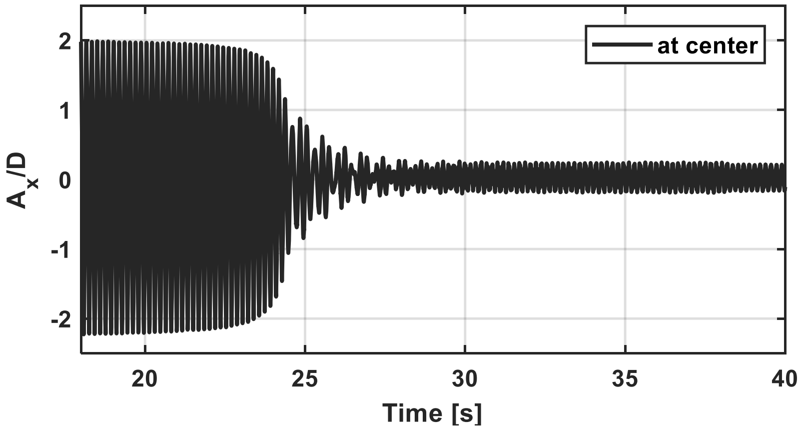

Fig. 6. Cylinder's center point amplitude response at center when the piezo is activated around 18 seconds, and deactivated around 30 seconds (shaker continues to oscillate).

3.2. Response in the recirculating flow channel

Similar to in-air experiments, same test cylinder was used in a recirculating flow channel. Fig. 7 illustrates the RMS amplitude response in cross-flow (top image) and in in-line (bottom image) for increasing and decreasing flow speeds. It should be remembered that, cylinder was designed to oscillate with first mode in cross-flow and up to third mode in in-line for the current Reynolds number range.

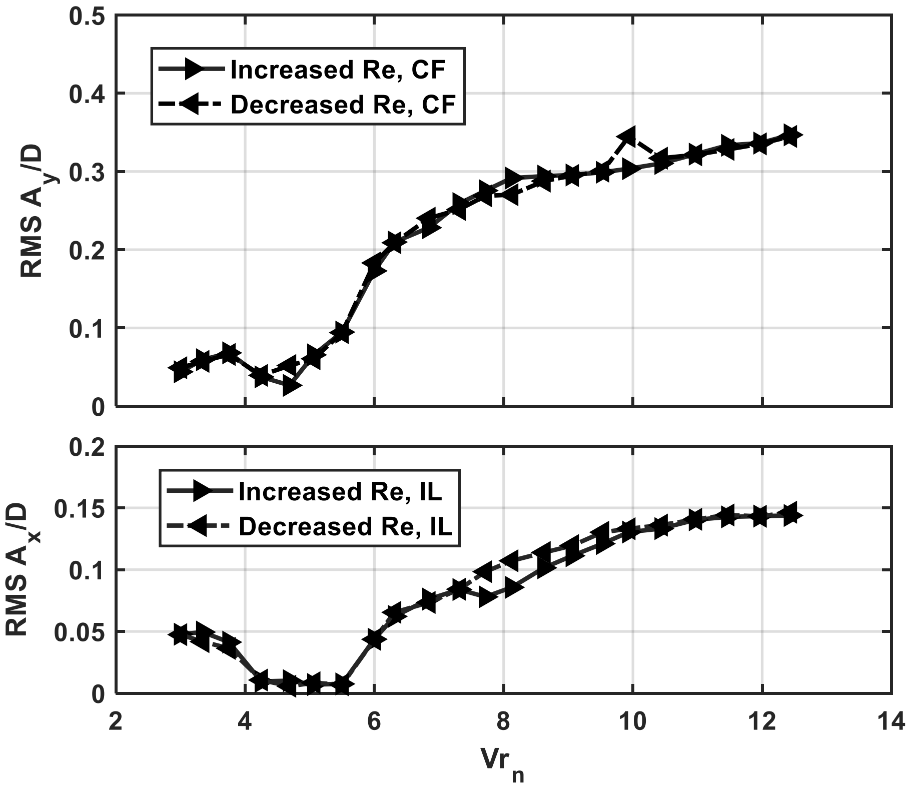

Fig. 7. RMS amplitude response in cross-flow (top image) and in in-line (bottom image).

Fig. 7 shows that cylinder oscillated with large in-line and cross-flow motions at low Reynolds numbers (until the normalized reduced velocity of 3.75), where the resulting mode shape was similar to first mode for both in-line and cross-flow directions. Then, a large amplitude drop was observed right after the reduced velocity of 3.75. Later, between the reduced velocities of 4 and 5.5, cylinder oscillated with very small in-line and small cross-flow motions. At this range, the resulting shape was similar to second mode in in-line and first mode in cross-flow. Some other interesting behaviors were observed at different flow speeds, but they are exempted from this paper for clarity.

3.3. Case Study: Controlling the motion at $Vr_n = 3.75$

RMS amplitude response in Fig. 7 showed that large amplitude drop occurred right after the normalized reduced velocity of 3.75. Therefore, the motion at this reduced velocity was chosen to test whether the piezos are capable of disrupting the frequency characteristics.

Fig. 8 illustrates the response at $Vr_n = 3.75$ where cylinder oscillated with similar to figure eight type of shape. Cross-flow oscillation frequency is computed as $6Hz$, which is close to the natural frequency, and in-line frequency is $3Hz$.

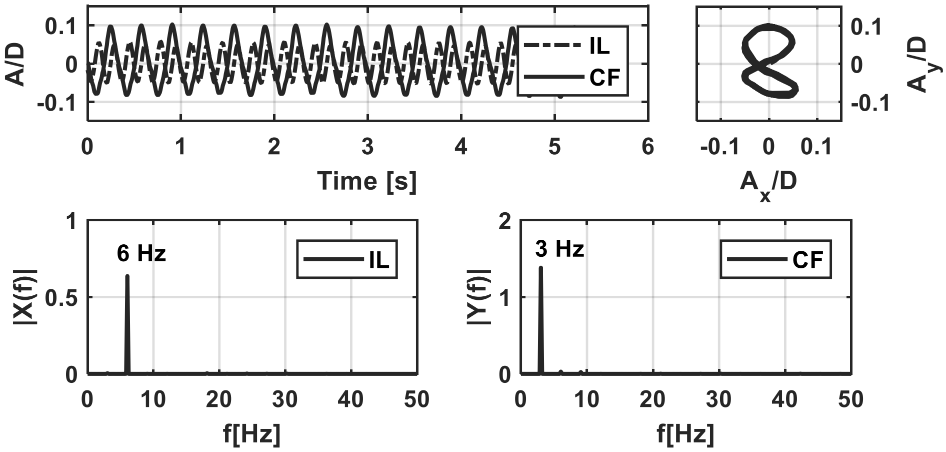

Fig. 8. Response at $Vr_n = 3.75$. Top left: Time history in in-line and cross-flow. Top right: Corresponding Lissajous shape. Bottom left: Frequency response in in-line at $L/4$ from the top. Bottom right: Frequency response in cross-flow at $L/4$ from the top.

Fig. 9 illustrates the piezo-activated response at the reduced velocity of 3.75 where piezo was activated around the piezo frequency of $40Hz$. As time history and Lissajous shape clearly illustrate, activating the piezo resulted a significant amplitude drop in both in-line and cross-flow directions. In this case, the amplitude drop was close to 75% in cross-flow direction and very small in-line response was observed in in-line. Frequency response plots in Fig. 9 also illustrated some interesting results. For example, activating the piezos increased the cross-flow frequency from 3 to $3.8Hz$, and forced cylinder to oscillate with $40Hz$ in in-line direction with active lower harmonics of $3.8Hz$ and $10Hz$.

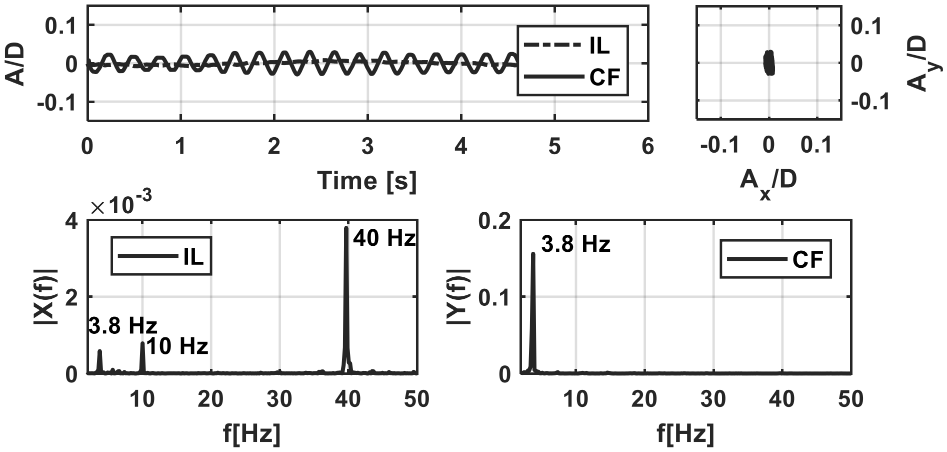

Fig. 9. Piezo activated response at $Vr_n = 3.75$. Top left: Time history in in-line and cross-flow. Top right: Corresponding Lissajous shape. Bottom left: Frequency response in in-line at $L/4$ from the top. Bottom right: Frequency response in cross-flow at $L/4$ from the top.

4. Conclusion

Results of this work show that it is possible to alter the frequency characteristics of the cylinder and force it to oscillate in another amplitude state. It is also found that the method works both in air and in water applications.

In the experiments, piezo patches were bonded in the in-line direction at the second mode anti-node of the cylinder. In-line direction was chosen for piezo attachment because cylinder inherently oscillates with lower amplitudes in in-line then cross-flow in vortex-induced vibrations.

In-air experiments showed that cylinder reached the maximum amplitude response when it oscillated close to the first mode cross-flow natural frequency of the cylinder. This condition is known as resonance condition. Then, it was shown that when the piezo was activated, cylinder’s frequency characteristics changed and amplitude dropped. Later, similar experiments were carried out in a recirculating flow channel where the flow speed was first increased and then decreased. RMS response amplitude plot showed that cylinder oscillated with similar to first mode shape until the reduced velocity of 3.75 and then the amplitude in in-line dropped significantly. Since an apparent amplitude drop occurred at this reduced velocity, this reduced velocity was chosen for illustration. At $Vr_n = 3.75$, cylinder oscillated with $3Hz$ in cross-flow and $6Hz$ in in-line, then piezos were activated with the maximum piezo frequency of $40Hz$. Frequency response plots showed that, piezo activation resulted a frequency increase in both directions where in-line frequency jumped from $6Hz$ to $40Hz$ (to the piezo frequency), and cross-flow frequency jumped from $3Hz$ to $3.8Hz$. This frequency alteration also resulted a mode change and a significant amplitude drop in both in-line and cross-flow motion of the body (75% in cross-flow only). Experiments were carried out four times to ensure that this response is a stable response at this flow speed.

In this study, we presented the response only at one flow speed in the recirculating flow channel as a representative of vibration suppression. However, other flow speeds were also analyzed and some other interesting results were observed. For example, it was observed that in addition to vibration suppression, vibration of the motion could also be increased significantly. In addition, piezo patches were found to be an active method for reducing the higher harmonics in the system. Although, these results are not presented here, they will be published in a journal article soon.

Nomenclature

$\frac{A_x}{D}, \frac{A_y}{D}$	Normalized amplitude in in-line (x) and in cross-flow (y)
Vr	Reduced velocity ($Vr = \frac{U}{fD}$)
Vr_n	Normalized reduced velocity ($Vr_n = \frac{U}{f_n D}$)
D	Cylinder diameter
L	Cylinder length
f	Oscillation frequency
f_n	Natural frequency
U	Nominal flow speed
Re	Reynolds number ($Re = \frac{UD}{v}$)
v	Kinematic viscosity of water
E	Modulus of elasticity
I	Area moment of inertia
M	Mass per unit length

Acknowledgement

The authors gratefully acknowledge support for this work from the Office of Naval Research (grant N00014-16-1-2968, PM Kelly Cooper).

References

Baz, A., Kim, M. (1993). Active modal control of vortex-induced vibrations of a flexible cylinder. Journal of Sound and Vibration 165 (1), 69-84

Bearman, P W. (1984). Vortex Shedding from Oscillating Bluff Bodies. Annual Review of Fluid Mechanics 16, no. 1: 195-222.

Blevins, R.D. (1990). Flow induced vibrations, 2nd edition. Van Nostrand Reinhold Company, New York, NY

Bourguet, R., Karnidiakis, G., and Triantafyllou, M. (2011). Vortex-induced vibrations of a long flexible cylinder in shear flow. Journal of Fluid Mechanics, vol. 677, pp. 342-382.

Chaplin, J.R., Bearman, P.W., Huera-Huarte, F.J., Pattenden, R.J. (2005). Laboratory measuruments of vortex-induced vibrations of a vertical tension riser in a stepped current. Journal of Fluids and Structures, 21, 3-24.

Cheng, L., Zhou, Y., Zhang, M. (2003). Perturbed interaction between vortex shedding and induced vibration. Journal of Fluids and Structures 17(7),887-901.

Dahl, J. M., Hover, F.S, and Triantafyllou, M.S. (2006). Two-Degree-of-Freedom Vortex-Induced Vibrations Using a Force Assisted Apparatus. J. of Fluids and Structures 22, no. 6: 807-18.

Dahl, J. M., Hover, F.S., Triantafyllou, M.S, Dong, S., and Karniadakis, G.E. (2007). Resonant Vibrations of Bluff Bodies Cause Multivortex Shedding and High Frequency Forces. Physical Review Letters 99, no. 14: 144503.

Gedikli, E.D., and Dahl, J.M. (2004). Mode Shape Variation for a Low-Mode Number Flexible Cylinder Subject to Vortex-Induced Vibrations. ASME 2014 33rd OMAE, no. 45400: V002T08A71.

Gedikli, E.D., and Dahl, J.M. (2017). Mode Excitation Hysteresis of a Flexible Cylinder Undergoing Vortex-Induced Vibrations. Journal of Fluids and Structures 69, no. Supplement C: 308-22.

Gedikli, E.D., Dahl J.M., and Chelidze, D. (2017). Multivariate Analysis of Vortex-Induced Vibrations in a Tensioned Cylinder Reveal Nonlinear Modal Interactions. Procedia Engineering 199, no. Supplement C: 546-51.

Huera-Huarte, F. J., and Bearman, P.W. (2009). Wake Structures and Vortex-Induced Vibrations of a Long Flexible Cylinder—Part 1: Dynamic Response. Journal of Fluids and Structures 25, no. 6: 969-90.

Huera-Huarte, F. J., Bangash, Z.A., and González, L.M. (2014**).** Towing Tank Experiments on the Vortex-Induced Vibrations of Low Mass Ratio Long Flexible Cylinders." Journal of Fluids and Structures 48, no. Supplement C: 81-92.

Jauvtis, N., and Williamson, C.H.K. (2004). The effect of two degrees of freedom on vortex-induced vibration at low mass and damping. Journal of Fluid Mechanics 509: 23-62.

Modarres-Sadeghi, Y., Mukundan, H., Dahl, J., Hover, F., and Triantafyllou, M. (2010). The effect of higher harmonic forces on fatigue life of marine risers, Journal of Sound and Vibration, vol. 329, no. 1, pp. 43-55.

Sarpkaya, T. (2004). A Critical Review of the Intrinsic Nature of Vortex-Induced Vibrations." Journal of Fluids and Structures 19, no. 4: 389-447.

Vandiver, J.K. (1993). Dimensionless parameters important to the prediction of vortex-induced vibration of long, flexible cylinders in ocean currents. Journal of Fluids and Structures. 7, 423-455.

Vandiver, J., Marcollo, H., Swithenbank, S., Jhingran, V. (2006). High-mode vortex-induced vibration field experiments. Jouranl of Pet. Technol. 58,69-70.

Williamson, C.H.K., and Govardhan R. (2004). Vortex-induced vibrations. Annual Review of Fluid Mechanics 36, no. 1: 413-55.

Williams, J.F., Zhao, B. (1989). The active control of vortex shedding. Journal of Fluids and Structures 3(2), 115-122.